


Geophysical Research Letters



RESEARCH LETTER

10.1029/2019GL086176

Atmospheric Freshwater Transport From the Atlantic to the Pacific Ocean: A Lagrangian Analysis

Dipanjan Dey¹  and Kristofer Döös¹ 

¹Department of Meteorology (MISU), Stockholm University, Stockholm, Sweden

Key Points:

- A new Lagrangian method to trace atmospheric freshwater is introduced based on water mass fluxes and not humid air
- Atlantic to Pacific atmospheric water mass transport was traced with Lagrangian trajectories
- The westerlies transport approximately twice as much water as the easterly trade winds

Supporting Information:

- Supporting Information S1

Correspondence to:

D. Dey,
dipanjan.dey@misu.su.se

Citation:

Dey, D., & Döös, K. (2020). Atmospheric freshwater transport from the Atlantic to the Pacific Ocean: A Lagrangian analysis. *Geophysical Research Letters*, 47, e2019GL086176. <https://doi.org/10.1029/2019GL086176>

Received 8 NOV 2019

Accepted 9 MAR 2020

Accepted article online 11 MAR 2020

Abstract The Atlantic-to-Pacific atmospheric freshwater transport was calculated using Lagrangian water mass trajectories. These were decomposed into eastward and westward moving classes, carrying water over Afro-Eurasia and over America, respectively. The results reveal that the midlatitude westerlies are contributing to midlatitude precipitation in the Pacific Ocean through transporting water mass from the midlatitude Atlantic Ocean over Afro-Eurasia. In addition, precipitation in the Eastern Tropical Pacific Ocean is found to be associated with the easterly winds carrying water mass from the tropical Atlantic Ocean. A quantitative analysis of the atmospheric freshwater transport furthermore shows that annually, the westerlies carry 0.40 Sv, approximately twice as much water as the easterly trade winds (0.26 Sv) to the Pacific Ocean, but with a strong seasonality. The Atlantic Ocean exports more freshwater across Afro-Eurasia than across America, except during the June–August periods. The average residence time of this atmospheric water transport is roughly twice as long when it crosses Afro-Eurasia (54 days) rather than America (24 days).

Plain Language Summary The Pacific Ocean is less saline than the Atlantic Ocean. This salinity difference feeds the Conveyor Belt, which transfers warm water from the Pacific Ocean to the Atlantic as a shallow current and returns cold water from the Atlantic to the Pacific as a deep current that flows further south. One explanation of this salinity difference is that the evaporation dominates over precipitation in the Atlantic and vice versa for the Pacific. This salinity asymmetry has often been believed to be due to the westward directed winds carrying the moisture over America. However, in the present study we show that the moisture transport by the eastward directed winds over Afro-Eurasia is also important. The present study reveals that the moisture export from the midlatitude Atlantic to the midlatitude Pacific Ocean over Afro-Eurasia by the eastward directed winds is approximately twice as large as the moisture export from the tropical Atlantic Ocean to the Eastern Tropical Pacific Ocean across America by the westward directed winds, except during the June–August periods. The moisture carried over Afro-Eurasia by the eastward directed winds from the Atlantic to the Pacific Ocean tends to take place at higher altitude and remains longer in the atmosphere than the moisture carried by the westward directed trade winds.

1. Introduction

Moisture export from the Atlantic to the Pacific Ocean through the atmosphere is one of the important contributing processes giving rise to the North Atlantic Deep Water (Richter & Xie, 2010) and thus also a key element for maintaining the Atlantic Meridional Overturning Circulation (MOC) as well as the entire Global Ocean Conveyor Belt. High sea surface temperatures lead to higher evaporation rates resulting in a larger moisture content in the atmosphere and salinification of the subtropical Atlantic Ocean (Czaja, 2009; Warren, 1983). This evaporated moisture is affected by easterly trade winds and is exported to the Pacific Ocean mainly across Central America (Levang & Schmitt, 2015). The warm, high-saline subtropical Atlantic waters are then transported by the prevailing ocean currents to higher latitudes, where they lose heat to the atmosphere (cooling) and sink down to a depth of approximately 2,000 m to form the North Atlantic Deep Water (Gordon & Piola, 1983; Gordon, 1986; Ferreira et al., 2018). A similar deep convective cell and a vigorous MOC are not found in the Pacific Ocean. Several hypotheses, including the effects of different basin geometries (Ferreira et al., 2010; Nilsson et al., 2013), the presence of multiple equilibria of the MOC (Huisman et al., 2009), interbasin salt transport (Weijer et al., 1999), and mountain-range configurations (Sinha et al., 2012) have been put forward to explain this asymmetry.

©2020. The Authors.

This is an open access article under the terms of the Creative Commons Attribution-NonCommercial License, which permits use, distribution and reproduction in any medium, provided the original work is properly cited and is not used for commercial purposes.

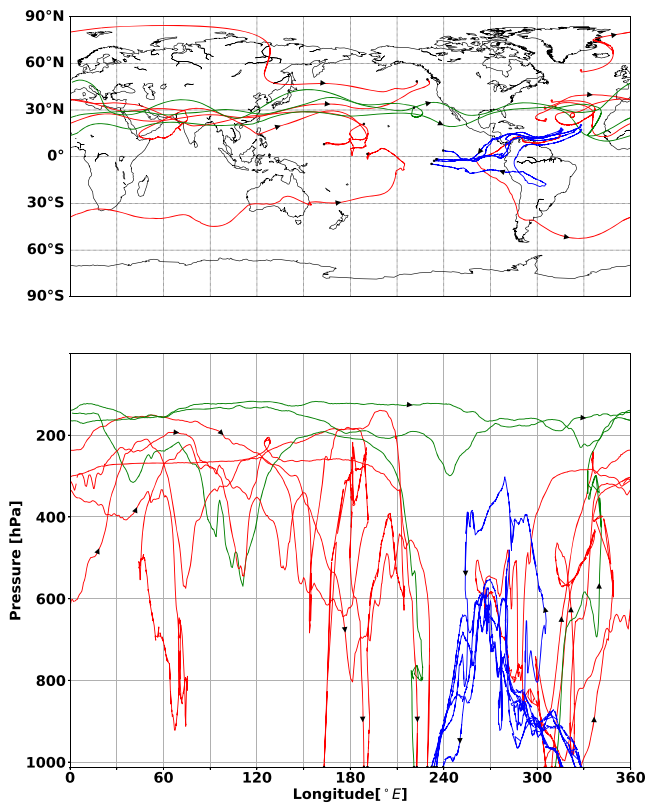


Figure 1. Selection of representative water mass trajectories starting at the surface of the Atlantic due to evaporation and followed until they “precipitate” in the Pacific Ocean. Westward moving over America in blue and eastward moving over Afro-Eurasia in red. One eastward moving trajectory in green circles around the world twice before precipitating in the Pacific.

Atmospheric freshwater forcing is an essential component involved in nearly all these hypotheses. The Pacific Ocean receives 0.40 Sv (1 Sv $\equiv 10^9$ kg/s) more atmospheric freshwater between 35°S and 60°N compared to the Atlantic Ocean (Craig et al., 2017), which explains half of the Atlantic-Pacific average salinity difference (one practical salinity unit). This asymmetry of the atmospheric freshwater forcing is primarily caused by the atmospheric eddies and monsoonal circulations. The stationary eddies in the atmosphere are responsible for the subpolar North Pacific freshening (exceeding that taking place in the subpolar North Atlantic) by giving rise to the Aleutian Low (Wills & Schneider, 2015).

The Pacific-Ocean basin receives atmospheric freshwater from its eastern and western boundaries. The path across the eastern boundary is mainly concentrated between 15°S to 20°N (Ferreira et al., 2018), where atmospheric moisture transports to the Pacific Ocean take place due to the easterly trade winds. The Monsoonal circulation contributes to the transport of moisture to the tropical and subtropical Pacific Ocean across its western boundary between 5°N and 25°N (Emile-Geay et al., 2003). The atmospheric influx of freshwater to the Pacific can come from any ocean basin, while that carried by ocean currents is constrained by land masses acting as lateral boundaries. A great deal of research has been conducted to quantify the net atmospheric freshwater transport from the Atlantic to the Pacific Ocean across Central America (Wang et al., 2013), but only limited studies have hitherto been carried out to calculate the actual freshwater transports from the Atlantic to the Pacific Ocean over Afro-Eurasia and the Americas, respectively. The aim of the present study is to calculate the atmospheric freshwater export from the Atlantic to the Pacific Ocean across its western (i.e., over America) and eastern (i.e., over Afro-Eurasia) boundaries and the associated atmospheric processes. This will be carried out using a Lagrangian-trajectory approach.

2. Atmospheric Water Mass Trajectories

TRACMASS (Döös, 1995), a Lagrangian trajectory model, was adapted for the present study to track freshwater in the atmosphere. In contrast to most other Lagrangian trajectory models, TRACMASS uses mass fluxes instead of velocities (Vries & Döös, 2001), which has made it possible to trace water-transport pathways in the ocean (Berglund et al., 2017; Döös et al., 2008) and air masses in the atmosphere (Kjellsson & Döös, 2012). A more detailed description of TRACMASS can be found in Döös et al. (2017).

In the present study TRACMASS has been further extended to trace water masses in the atmosphere. A detailed evaluation has been carried out of the atmospheric water mass version of TRACMASS Lagrangian model (see the supporting information). It is important to note here that we are not tracing air including moisture but the actual water mass transport itself. A detailed derivation of this 3-D atmospheric water mass flux field is provided in Appendix A, where the vertical component is computed from a water mass continuity equation. Due to water mass conservation, this vertical water mass flux will not only include the advection of water vapor but also a vertical water mass transport consisting of liquid water and ice. Note that this could either be precipitation, if downward, or re-evaporation of precipitation, which typically occurs in clouds.

Note that in the present study, atmospheric “water masses” instead of “humid air masses” were traced from the net evaporative surface to the net precipitating surface using a 3-D atmospheric water mass flux field. This would not have been possible by tracing humid air since there is no air flux through the surface, but here we trace water, which has a flux through the surface due to evaporation and precipitation. Thus, this mass conserving Lagrangian algorithm will not use any “well-mixed” assumptions (Tuinenburg et al., 2012), which can lead to errors in regions of large wind shear (Van der Ent et al., 2013). Also, the present Lagrangian method does not assume a constant mass of the atmosphere (Stohl & James, 2004), which may ultimately not hold for synoptic time scales.

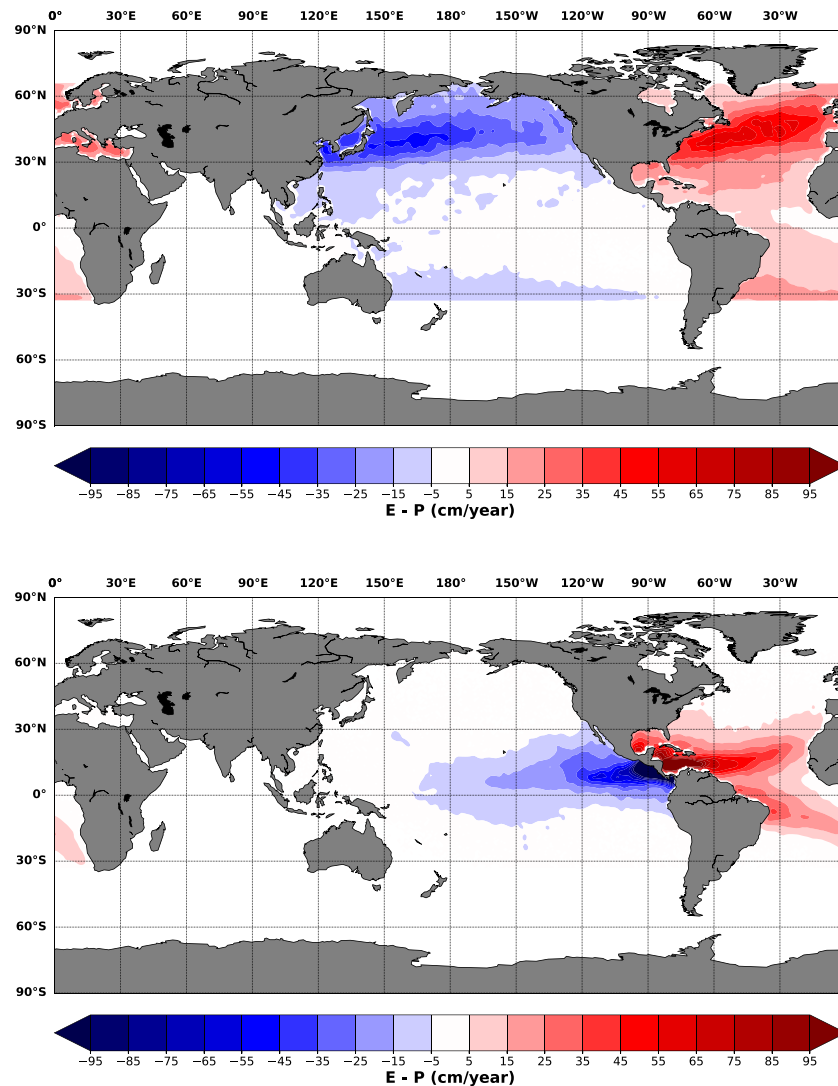


Figure 2. E-P inferred from the water mass traveling from the Atlantic to Pacific Ocean over Afro-Eurasia (top) and America (bottom). Note that this is not the same as the total E-P since this flux is only due to the Atlantic-to-Pacific atmospheric water transport.

Atmospheric water mass fluxes were computed using the ERA-Interim's specific humidity, surface pressure, and horizontal wind velocities at each vertical model level (Dee et al., 2011). The data were extracted for the years 2016 and 2017 with 0.75° horizontal resolution and 60 hybrid vertical levels. Temporal resolution of the extracted data was 6 hr. The state of the art observationally based reanalysis product ERA-Interim uses four-dimensional variational analysis for data assimilation. In addition, a revised humidity analysis was also incorporated in ERA-Interim to improve the representation of the water cycle compared to its precursor ERA-40. It also handles better the biases and changes in the observing system through variational bias correction method. This makes ERA-Interim suitable for the present study. Note that the majority of the atmospheric reanalysis data sets are implicitly incorporating atmospheric water mass modifications in the surface pressure analysis (Bosilovich et al., 2017). To be able to match with the observations, assimilation schemes try to adjust model atmosphere by adding/removing moisture. Thus, water budget in the reanalysis data sets is not needed to be in perfect balance (Trenberth & Smith, 2005).

3. Results

3.1. Atmospheric Water Mass Transport From the Atlantic to the Pacific Ocean

As the Atlantic Ocean is a net evaporative basin (Bryan & Oort, 1984; Jacobs, 1949), aerial-moisture export is a major mechanism to maintain its high sea surface salinity. To calculate the water mass transport from

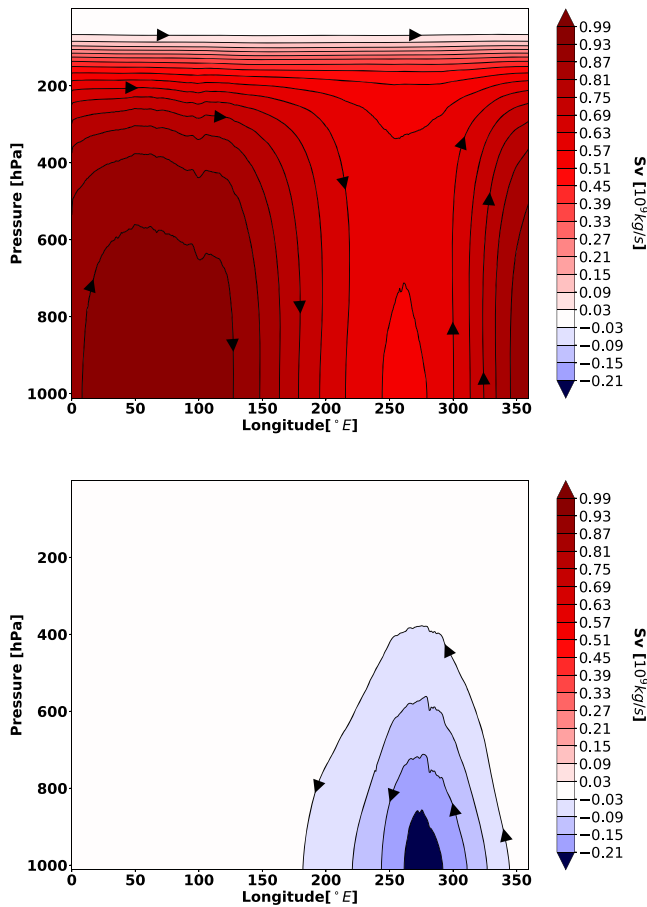


Figure 3. Atmospheric zonal water mass stream function (Sv), constructed from the water mass traveling from the Atlantic to Pacific Ocean over Afro-Eur-Asia (top) and America (bottom).

containing the Atlantic to the Pacific Ocean through the atmosphere, the Lagrangian “particles” over the entire Atlantic were assigned to the vertical water mass flux at the surface (viz., evaporation-precipitation). The particles were started at the surface, where evaporation exceeds precipitation, and end at the surface where the opposite holds true. As the aim of the present study is to examine the atmospheric water mass transport from the Atlantic to the Pacific Ocean, we have only selected those trajectories (around 4.3 million) that descended into the Pacific Ocean (Figure 1). The total continental runoff into the Pacific is about 0.25 Sv according to Dai and Trenberth (2002). This total continental runoff has moisture contributions from its local sources, from different oceans and land sources. Thus, only Atlantic contribution to this runoff is likely to be much smaller. This continental runoff into the Pacific Ocean has thus been neglected in the present calculation. Figure 1 displays a selection of Atlantic-to-Pacific trajectories showing the two different possible paths: one over Afro-Eurasia (red) and one over America (blue). Some of the trajectories (green) were trapped in the westerlies and circled around the globe a few times before precipitating down into the Pacific. It is important to emphasize here that we are not taking into account the water mass trajectories that start and end in the Atlantic Ocean.

3.1.1. Over Afro-Eurasia

Figure 2 (top) displays the annual mean E-P (evaporation-precipitation) inferred from the eastward traveling Lagrangian particles from the Atlantic Ocean. As the TRACMASS Lagrangian scheme is based on the mass-conservation principle, from the extracted trajectories the integrated value of net evaporation over the Atlantic Ocean should equal the integrated value of net precipitation over the Pacific Ocean. Figure 2 (top) shows the net precipitation flux in the midlatitude North Pacific Ocean due to evaporation in the midlatitude North Atlantic Ocean. As the core of the evaporative region is not located in the tropical latitudes, the water mass particles starting from the higher latitudes of the North Atlantic Ocean come under the influence of the subtropical westerlies and travel eastward. Then the trajectories cross the African, European, and Asian continents and finally descend into the Pacific Ocean. Note that the Western Pacific Warm Pool receives very little freshwater from the Atlantic, despite it being a region with high precipitation. The Lagrangian water mass stream function (Figure 3, top) provides information about the paths in the vertical-zonal direction. The water mass streamlines start in the net evaporative regions in the Atlantic and travel eastward at heights between 600 and 100 hPa and end up in the Pacific. Note that some of the particles remained in the westerlies above 200 hPa and circled the globe a few times before precipitating. The seasonal pattern of this eastward atmospheric water transport can be obtained by subtracting the maximum value of the stream function at the surface from its minimum value (Figure 4, red line) for each month. The annual mean freshwater transport was found to be 0.40 Sv from the Atlantic to the Pacific Ocean over Afro-Eurasia. During the Northern Hemisphere summer, this transport decreased. This characteristic of the atmospheric water mass transport can be explained by the behavior of the midlatitude zonal winds. Their annual mean is westerly, and they are stronger during winter. The atmospheric water residence time has always been a crucial component of the global hydrological cycle. Figure 5 (red line) depicts the percentage of the eastward moving water mass present in the domain against time. From this, we can calculate an *e*-folding time, which represents a time scale in which the water masses decay by 63%. The *e*-folding time was estimated to be around 43 days for the eastward traveling trajectories. The average

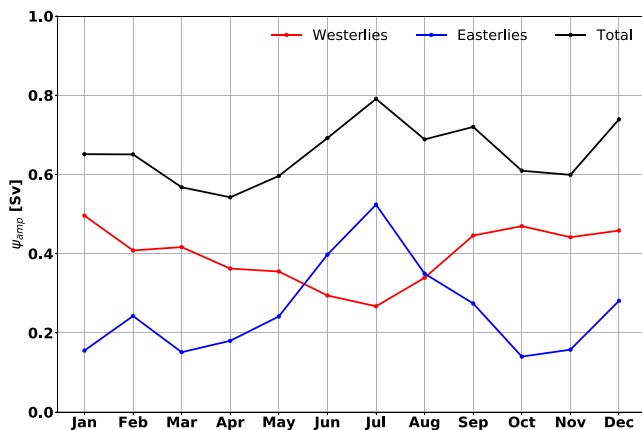


Figure 4. Atmospheric freshwater transport as a function of month computed from the water mass traveling from the Atlantic to Pacific Ocean over Afro-Eurasia by the westerlies (red) and over America by the easterlies (blue). The total atmospheric freshwater transport is plotted in black.

only the Atlantic to the Pacific Ocean through the atmosphere, the Lagrangian “particles” over the entire Atlantic were assigned to the vertical water mass flux at the surface (viz., evaporation-precipitation). The particles were started at the surface, where evaporation exceeds precipitation, and end at the surface where the opposite holds true. As the aim of the present study is to examine the atmospheric water mass transport from the Atlantic to the Pacific Ocean, we have only selected those trajectories (around 4.3 million) that descended into the Pacific Ocean (Figure 1). The total continental runoff into the Pacific is about 0.25 Sv according to Dai and Trenberth (2002). This total continental runoff has moisture contributions from its local sources, from different oceans and land sources. Thus, only Atlantic contribution to this runoff is likely to be much smaller. This continental runoff into the Pacific Ocean has thus been neglected in the present calculation. Figure 1 displays a selection of Atlantic-to-Pacific trajectories showing the two different possible paths: one over Afro-Eurasia (red) and one over America (blue). Some of the trajectories (green) were trapped in the westerlies and circled around the globe a few times before precipitating down into the Pacific. It is important to emphasize here that we are not taking into account the water mass trajectories that start and end in the Atlantic Ocean.

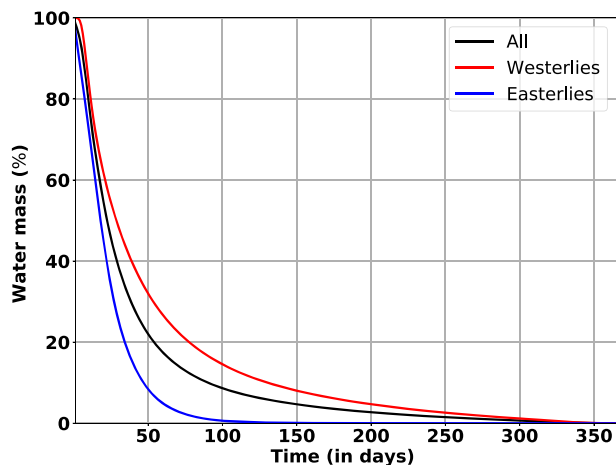


Figure 5. Atmospheric water residence time inferred from the water mass traveling from the Atlantic to Pacific Ocean over Afro-Eurasia by the westerlies (red) and over America by the easterlies (blue). The atmospheric water residence time constructed from all the water masses (water masses transported by both the westerlies and easterlies) traveling from the Atlantic to Pacific Ocean is graphed in black.

seasonal pattern of this westward water mass transport (Figure 4, blue line) indicates that the maximum transport (0.50 Sv) by the easterlies occurred during the summer month of July and that the transport is much smaller during the winter season. The northward movement of the Intertropical Convergence Zone, midsummer drought, variations of the coastal low-level jet, and intrusions of the North Atlantic High can explain this large water mass transport across America (Wang et al., 2013). Except during summer, the total water mass transport from the Atlantic to the Pacific Ocean was dominated by the westerlies; namely, it takes place over Afro-Eurasia. The annual mean atmospheric water transport over America by the easterly trade winds was found to be 0.26 Sv. This estimate matches reasonably well with the observational net Eulerian estimate of 0.36 Sv by Zaucker and Broecker (1992). The mean total atmospheric freshwater transport from the Atlantic to the Pacific Ocean was found to be 0.65 Sv. For westward traveling trajectories (Figure 5, blue line), the e -folding time was around 24 days, which is almost the same as their average residence time scale. The eastward moving water masses are associated with longer residence times because the trajectories sometime circle the Earth one or several times. Considering the trajectories together without dividing them into separate classes, the e -folding time was found to be 32 days (Figure 5, black line). The average residence time for the total atmospheric water masses traveling from the Atlantic to the Pacific Ocean was estimated to be approximately 41 days.

4. Discussion and Conclusions

There are different arguments regarding the origin of atmospheric moisture from the Atlantic Ocean and how this atmospheric freshwater is transported to the Pacific Ocean. Previous Eulerian estimates based on reanalyses of net vertically integrated zonal moisture fluxes across the Atlantic drainage basin suggest that the net zonal import across Africa (0.27 Sv in Levang & Schmitt, 2015, and 0.29 Sv in Singh et al., 2016) is largely surpassed by the net zonal export across Central America (0.40 Sv in Levang & Schmitt, 2015, and 0.46 Sv in Singh et al., 2016). The net import of atmospheric moisture into the Atlantic drainage basin across North America between 20°N and 70°N is almost balanced by the net zonal moisture export across Europe (Singh et al., 2016). It was thus believed that the Atlantic Ocean mainly exports its moisture across Central America. But from these calculations, it was difficult to quantify actual eastward freshwater transport (not net transport) from the Atlantic to the Pacific Ocean through the atmosphere. Also, sometimes, these Eulerian net zonal moisture flux calculations can be misleading as a large eastward moisture export can be partly compensated for by the westward moisture import.

In the present study, a Lagrangian approach was adopted to quantify the actual atmospheric freshwater transport from the Atlantic to the Pacific Ocean. Net moisture export from the Atlantic Ocean across America

water residence time was also computed (see the supporting information) for these classes of trajectories, and it was found to be approximately 54 days. It is important to note here that these times should not be compared with the global residence time of water in the atmosphere, which is much shorter and is provided in the supporting information. The reason for the long residence time for this eastward traveling water is that it requires a minimum time to cross Afro-Eurasia, while the global residence time includes the shorter regional and local residence times as well. Using a moisture-tracking algorithm, Van Der Ent and Tuinenburg (2017) also showed that the average age of the atmospheric water differs spatially and temporally. These researchers also found very high average water residence time in the atmosphere during the summer season in the Northern Hemisphere (see the supplementary animation video of Van Der Ent & Tuinenburg, 2017).

3.1.2. Over America

Figure 2 (bottom) indicates the annual mean E-P pattern constructed from the westward moving Lagrangian water particles. This shows that the water evaporating from the subtropical Atlantic Ocean is to a large extent advected by the easterly trade winds over America and precipitates in the Eastern Tropical Pacific. This westward path does not ascend as high as the eastward path (Figure 3, bottom). It is generally confined below 400 hPa, and no particles remain stuck in the easterlies. The seasonal pattern of this westward water mass transport (Figure 4, blue line) indicates that the maximum transport (0.50 Sv) by the easterlies occurred during the summer month of July and that the transport is much smaller during the winter season.

has in previous studies been estimated to range from 0.20 to 0.40 Sv. We have only computed the transport from the Atlantic, which in the westward case over America was 0.26 Sv. This could fit the previous net estimates, but only if the net transport is between 0.20 and 0.26 Sv. In earlier studies, the net moisture export across Europe between 20°N and 70°N was found to be 0.26 Sv (Singh et al., 2016), and net westward moisture import across Africa into the Atlantic basin between 15°S and 20°N was found to be around 0.29 Sv. The atmospheric water export across Afro-Eurasia from the Atlantic to the Pacific Ocean was found to be 0.40 Sv based on the present Lagrangian analysis. Note that the results from the previous studies were based on the net Eulerian flux calculations, so actual eastward atmospheric freshwater transport cannot be obtained, and furthermore, these flux computations were based on moisture sources, which were indistinguishable. In addition, the discrepancy between the Eulerian and Lagrangian transport estimates over Afro-Eurasia may be reinforced because of the moisture import to the Atlantic Ocean from the different moisture sources, which were not taken into account in our Lagrangian computation. Inspection of seasonal atmospheric freshwater transports reveals that the moisture export across Afro-Eurasia was always larger than the moisture export across America except during the months from June to August. The annual mean total atmospheric freshwater export from the Atlantic to the Pacific Ocean was found to be 0.65 Sv based on the present Lagrangian approach. The water mass exported by the westerlies has a higher e -folding residence time (43 days) than the water mass transported by the easterly trade winds (24 days).

The present Lagrangian water mass transport method could provide an additional way to compare different reanalysis data sets as well as various Earth system models. This novel constraint will therefore show differences that were not visible in the traditional Eulerian comparisons (e.g., Yu et al., 2017). It is not possible to observe directly the interocean exchange of atmospheric freshwater. We have, however, computed the net E-P from the water mass trajectories and compared that with the ERA-Interim (see the supporting information). This is the only way to validate its robustness although it is not comparing directly the freshwater transports. Note that the atmospheric freshwater transport magnitude and residence time estimates presented here depend on the used reanalysis product. Most of the observationally based atmospheric reanalysis products have nonidentical horizontal and vertical resolutions and use different parameterization and assimilation schemes; these will definitely have impacts on the magnitudes of the diagnostics documented. The atmospheric water transport and residence time assessments obtained in the present study from the reanalysis data could also serve to identify biases between the current-generation global climate models (GCMs) within the Coupled Model Intercomparison Project. It is also noteworthy here that the GCMs used in Coupled Model Intercomparison Project solve a moisture tracer equation, which conserves water mass and should hence have an internally balanced hydrological cycle. But Liepert and Lo (2013) showed that only few GCMs have balanced water cycle and others were suffering from nonphysical sources/sinks of atmospheric moisture. Therefore, while using GCM data for atmospheric water transport studies, hydrological cycle representation check is important. Otherwise, it could lead to some unrealistic results.

The present atmospheric water mass transport study could be further extended to establish a freshwater connectivity between all the ocean basins (including the continental runoff) through the atmosphere. Another possible extension would be to include the oceanic counterpart of this interocean exchange of freshwater using Lagrangian trajectories in order to describe the full hydrological cycle. This analysis can also be used to trace specific phenomena such as the Monsoonal flow, which can be useful for countries like India, where agriculture and economy to a large extent depend upon the Monsoon. In conclusion, we hope that the new method presented here will be used in many other studies related to water mass tracking and residence-time estimates. This could also apply to the ocean, where heat and salt might be traced in the same way.

Appendix A: Lagrangian Water Mass Transport Calculation

The method is based on water mass conservation in the atmospheric circulation model and includes not only advection of moisture by the winds but also the vertical water mass transport due to evaporation and precipitation (Dey & Döös, 2019). To calculate the atmospheric water mass in a model grid box, we have multiplied its air mass with its specific humidity:

$$M_{i,j,k}^n = q_{i,j,k}^n \rho_{i,j,k}^n \Delta x_{i,j} \Delta y_{i,j} \Delta z_{i,j,k}^n, \quad (\text{A1})$$

where the superscript n represents the time level of the stored model fields; time is $t = n\Delta t_G$, where Δt_G is the time interval between two stored model fields. The longitudinal ($\Delta x_{i,j}$) and the latitudinal ($\Delta y_{i,j}$) grid

lengths are functions of their horizontal locations i, j . The vertical coordinate in the model has a level thickness $\Delta z_{i,j,k}^n$, where the subscript k denotes the vertical level. The specific humidity $q_{i,j,k}$ and density $\rho_{i,j,k}$ are functions of both the horizontal locations i, j and the vertical level k . The advective horizontal water mass transports through the eastern (U) and northern (V) faces of the (i, j, k) grid box at time step n are

$$U_{i,j,k}^n = q_{i,j,k}^n \rho_{i,j,k}^n u_{i,j,k}^n \Delta y_{i,j} \Delta z_{i,j,k}^n, \quad (\text{A2})$$

$$V_{i,j,k}^n = q_{i,j,k}^n \rho_{i,j,k}^n v_{i,j,k}^n \Delta x_{i,j} \Delta z_{i,j,k}^n, \quad (\text{A3})$$

Since the circulation model is hydrostatic, we may write

$$\Delta p_{i,j,k}^n = \rho_{i,j,k}^n g \Delta z_{i,j,k}^n, \quad (\text{A4})$$

where g is gravity and Δp is level thickness. The advective water mass transports through the lateral grid faces given by equations (A2) and (A3) will make use of equation (A4) to determine Δz and hence become

$$U_{i,j,k}^n = q_{i,j,k}^n u_{i,j,k}^n \Delta y_{i,j} \Delta p_{i,j,k}^n / g, \quad (\text{A5})$$

$$V_{i,j,k}^n = q_{i,j,k}^n v_{i,j,k}^n \Delta x_{i,j} \Delta p_{i,j,k}^n / g. \quad (\text{A6})$$

Conservation of water mass yields that the rate of change of the water mass content of a box balances the water mass fluxes through its faces:

$$\frac{\partial M_{i,j,k}}{\partial t} + U_{i,j,k} - U_{i-1,j,k} + V_{i,j,k} - V_{i,j-1,k} + W_{i,j,k} - W_{i,j,k-1} = 0, \quad (\text{A7})$$

where $W_{i,j,k}$ is the vertical water mass transport through the upper face of the grid box. Equation (A7) can be rewritten by discretizing the time derivative and using the hydrostatic approximation (equation (A4)):

$$\frac{(\Delta p_{i,j,k}^n q_{i,j,k}^n - \Delta p_{i,j,k}^{n-1} q_{i,j,k}^{n-1})}{g \Delta t_G} \Delta x_{i,j} \Delta y_{i,j} + U_{i,j,k}^n - U_{i-1,j,k}^n + V_{i,j,k}^n - V_{i,j-1,k}^n + W_{i,j,k}^n - W_{i,j,k-1}^n = 0. \quad (\text{A8})$$

Values of W at all vertical levels can be computed by integrating equation (A8) downward from the top of the atmosphere (TOA), where the vertical water mass transport is close to zero. The vertical water mass flux is hence always computed at the bottom of each grid box successively downward:

$$W_{i,j,k-1}^n = W_{i,j,k}^n + \left[U_{i,j,k}^n - U_{i-1,j,k}^n + V_{i,j,k}^n - V_{i,j-1,k}^n + \frac{(\Delta p_{i,j,k}^n q_{i,j,k}^n - \Delta p_{i,j,k}^{n-1} q_{i,j,k}^{n-1})}{g \Delta t_G} \Delta x_{i,j} \Delta y_{i,j} \right]. \quad (\text{A9})$$

At the surface $W_{i,j,0}^n$ should be equal to evaporation-precipitation ($E - P$). The calculation of the water mass flux only omits the horizontal advection of liquid water and ice; however, their phase transitions into vapor form were taken into account. In addition, the transition from vapor to liquid water and ice was also included. The assumption of neglecting horizontal transport of ice and liquid water in a Lagrangian moisture tracking scheme has no significant impact on their results (Van der Ent et al., 2013).

The TRACMASS trajectory scheme (Döös et al., 2017) calculates water mass trajectories based on the Eulerian water mass fluxes computed above, (viz., $U_{i,j,k}^n, V_{i,j,k}^n, W_{i,j,k}^n$). A Lagrangian zonal overturning stream function was computed following Döös et al. (2008):

$$\psi_{i,k}^L = \sum_{k'=0}^k \sum_j \sum_n F_{i,j,k',n}^x, \quad (\text{A10})$$

where $F_{i,j,k',n}^x$ is the Lagrangian zonal atmospheric water mass transport by the trajectory index n through the meridional-vertical grid box wall.

Acknowledgments

The authors wish to thank Peter Lundberg for constructive comments. We are grateful for discussions on this work with Aitor Aldama Campino and Sara Berglund. In addition, the lead author wish to acknowledge Saikat Dey for his help to make the Plain Language Summary really plain. The ERA-Interim data used in this study are freely available from the ECMWF (<https://www.ecmwf.int/en/forecasts/datasets/archive-datasets/reanalysis-datasets/era-interim>). The TRACMASS trajectory model can be downloaded from <https://github.com/TRACMASS>. The Lagrangian trajectory model outputs are available at <https://doi.org/10.5281/zenodo.3478500>. The TRACMASS model integrations and the Lagrangian stream function computations were performed on resources provided by the Swedish National Infrastructure for Computing (SNIC) at the National Supercomputer Centre at Linköping University (NSC).

References

- Berglund, S., Döös, K., & Nycander, J. (2017). Lagrangian tracing of the water-mass transformations in the Atlantic Ocean. *Tellus A: Dynamic Meteorology and Oceanography*, *69*(1), 1306311.
- Bosilovich, M. G., Robertson, F. R., Takacs, L., Molod, A., & Mocko, D. (2017). Atmospheric water balance and variability in the MERRA-2 reanalysis. *Journal of Climate*, *30*(4), 1177–1196.
- Bryan, F., & Oort, A. (1984). Seasonal variation of the global water balance based on aerological data. *Journal of Geophysical Research*, *89*(D7), 11,717–11,730.
- Craig, P. M., Ferreira, D., & Methven, J. (2017). The contrast between atlantic and pacific surface water fluxes. *Tellus A: Dynamic Meteorology and Oceanography*, *69*(1), 1330454.
- Czaja, A. (2009). Atmospheric control on the thermohaline circulation. *Journal of Physical Oceanography*, *39*(1), 234–247.
- Dai, A., & Trenberth, K. E. (2002). Estimates of freshwater discharge from continents: Latitudinal and seasonal variations. *Journal of Hydrometeorology*, *3*(6), 660–687.
- Dee, D. P., Uppala, S. M., Simmons, A., Berrisford, P., Poli, P., Kobayashi, S., et al. (2011). The ERA-Interim reanalysis: Configuration and performance of the data assimilation system. *Quarterly Journal of the Royal Meteorological Society*, *137*(656), 553–597.
- Dey, D., & Döös, K. (2019). The coupled ocean-atmosphere hydrologic cycle. *Tellus A: Dynamic Meteorology and Oceanography*, *71*(1), 1–11.
- Döös, K. (1995). Inter-ocean exchange of water masses. *Journal of Geophysical Research*, *100*(C7), 13,499–13,514.
- Döös, K., Jönsson, B., & Kjellsson, J. (2017). Evaluation of oceanic and atmospheric trajectory schemes in the TRACMASS trajectory model v6.0. *Geoscientific Model Development*, *10*(4), 1733–1749.
- Döös, K., Nycander, J., & Coward, A. C. (2008). Lagrangian decomposition of the Deacon cell. *Journal of Geophysical Research*, *113*, C07028. <https://doi.org/10.1029/2007JC004351>
- Emile-Geay, J., Cane, M. A., Naik, N., Seager, R., Clement, A. C., & van Geen, A. (2003). Warren revisited: Atmospheric freshwater fluxes and “why is no deep water formed in the North Pacific” *Journal of Geophysical Research*, *108*(C6), 3178. <https://doi.org/10.1029/2001JC001058>
- Ferreira, D., Cessi, P., Coxall, H. K., De Boer, A., Dijkstra, H. A., Drijfhout, S. S., et al. (2018). Atlantic-pacific asymmetry in deep water formation. *Annual Review of Earth and Planetary Sciences*, *46*, 327–352.
- Ferreira, D., Marshall, J., & Campin, J.-M. (2010). Localization of deep water formation: Role of atmospheric moisture transport and geometrical constraints on ocean circulation. *Journal of Climate*, *23*(6), 1456–1476.
- Gordon, A. L. (1986). Inter-ocean exchange of thermocline water. *Journal of Geophysical Research*, *91*(C4), 5037–5046.
- Gordon, A. L., & Piola, A. R. (1983). Atlantic Ocean upper layer salinity budget. *Journal of Physical Oceanography*, *13*(7), 1293–1300.
- Huisman, S., Dijkstra, H., von Der Heydt, A., & De Ruijter, W. (2009). Robustness of multiple equilibria in the global ocean circulation. *Geophysical Research Letters*, *36*, L01610. <https://doi.org/10.1029/2008GL036322>
- Jacobs, W. C. (1949). The distribution and some effects of the seasonal quantities of E-P (evaporation minus precipitation) over the North Atlantic and North Pacific. *Archiv für Meteorologie, Geophysik und Bioklimatologie, Serie A*, *2*(1), 1–16.
- Kjellsson, J., & Döös, K. (2012). Lagrangian decomposition of the Hadley and Ferrel cells. *Geophysical Research Letters*, *39*, L15807. <https://doi.org/10.1029/2012GL052420>
- Levang, S. J., & Schmitt, R. W. (2015). Centennial changes of the global water cycle in CMIP5 models. *Journal of Climate*, *28*(16), 6489–6502.
- Liepert, B. G., & Lo, F. (2013). CMIP5 update of “inter-model variability and biases of the global water cycle in CMIP3 coupled climate models” *Environmental Research Letters*, *8*(2), 29401.
- Nilsson, J., Langen, P. L., Ferreira, D., & Marshall, J. (2013). Ocean basin geometry and the salinification of the Atlantic Ocean. *Journal of Climate*, *26*(16), 6163–6184.
- Richter, I., & Xie, S.-P. (2010). Moisture transport from the atlantic to the Pacific basin and its response to North Atlantic cooling and global warming. *Climate Dynamics*, *35*(2-3), 551–566.
- Singh, H. K., Donohoe, A., Bitz, C. M., Nusbaumer, J., & Noone, D. C. (2016). Greater aerial moisture transport distances with warming amplify interbasin salinity contrasts. *Geophysical Research Letters*, *43*, 8677–8684. <https://doi.org/10.1002/2016GL069796>
- Sinha, B., Blaker, A. T., Hirschi, J. J.-M., Bonham, S., Brand, M., Josey, S., et al. (2012). Mountain ranges favour vigorous atlantic meridional overturning. *Geophysical Research Letters*, *39*, L02705. <https://doi.org/10.1029/2011GL050485>
- Stohl, A., & James, P. (2004). A Lagrangian analysis of the atmospheric branch of the global water cycle. Part I: Method description, validation, and demonstration for the August 2002 flooding in central Europe. *Journal of Hydrometeorology*, *5*(4), 656–678.
- Trenberth, K. E., & Smith, L. (2005). The mass of the atmosphere: A constraint on global analyses. *Journal of Climate*, *18*(6), 864–875.
- Tuinenburg, O., Hutjes, R., & Kabat, P. (2012). The fate of evaporated water from the ganges basin. *Journal of Geophysical Research*, *117*, D01107. <https://doi.org/10.1029/2011JD016221>
- Van Der Ent, R. J., & Tuinenburg, O. A. (2017). The residence time of water in the atmosphere revisited. *Hydrology and Earth System Sciences*, *21*(2), 779–790.
- Van der Ent, R., Tuinenburg, O., Knoche, H. R., Kunstmann, H., & Savenije, H. (2013). Should we use a simple or complex model for moisture recycling and atmospheric moisture tracking? *Hydrology and Earth System Sciences*, *17*, 4869–4884.
- Vries, P., & Döös, K. (2001). Calculating Lagrangian trajectories using time-dependent velocity fields. *Journal of Atmospheric and Oceanic Technology*, *18*(6), 1092–1101.
- Wang, C., Zhang, L., & Lee, S.-K. (2013). Response of freshwater flux and sea surface salinity to variability of the Atlantic warm pool. *Journal of Climate*, *26*(4), 1249–1267.
- Warren, B. A. (1983). Why is no deep water formed in the North Pacific? *Journal of Marine Research*, *41*(2), 327–347.
- Weijer, W., de Ruijter, W. P., Dijkstra, H. A., & Van Leeuwen, P. J. (1999). Impact of interbasin exchange on the atlantic overturning circulation. *Journal of Physical Oceanography*, *29*(9), 2266–2284.
- Wills, R. C., & Schneider, T. (2015). Stationary eddies and the zonal asymmetry of net precipitation and ocean freshwater forcing. *Journal of Climate*, *28*(13), 5115–5133.
- Yu, L., Jin, X., Josey, S. A., Lee, T., Kumar, A., Wen, C., & Xue, Y. (2017). The global ocean water cycle in atmospheric reanalysis, satellite, and ocean salinity. *Journal of Climate*, *30*(10), 3829–3852.
- Zaucker, F., & Broecker, W. S. (1992). The influence of atmospheric moisture transport on the fresh water balance of the atlantic drainage basin: General circulation model simulations and observations. *Journal of Geophysical Research*, *97*(D3), 2765–2773.